Solar energy for low carbon buildings: choice of systems for minimal installation area, cost, and environmental impact

Renhua Liu[1], Guoqing He[1,2]*, Yujie Su[1], Yi Yang[3] and De Ding[3]

*Correspondence:
Guoqinghe@zju.edu.cn

[1] College of Civil Engineering
and Architecture, Zhejiang
University, Hangzhou 310058,
China
[2] Center for Balance
Architecture, Zhejiang University,
Hangzhou 310058, China
[3] The Architectural Design
and Research Institute
of Zhejiang University Limited
Company, Hangzhou 310058,
China

Abstract

Solar application in buildings is limited by available installation areas. The performance of photovoltaic (PV) and solar collectors are compared in meeting the heating and cooling demand of a residential house using 100% solar energy through TRNSYS modelling of five systems that use air source heat pump and seasonal energy storage as optional assisting technologies. The results show that in a large scale, the PV working with air source heat pump is more efficient than the solar collector system. However, the photovoltaic/thermal (PV/T) is the most spatially efficient with an energy capacity of 551 kWh/m², 10.6% higher than that of the PV. Compared with the air source heat pump heating system using grid power, using solar energy regardless of system formats can reduce emission by 72% in a lifetime of 20 years. Solar energy can become cost-effective if the utility price is increased to above 0.7 CNY/kWh. The results can help in renewable planning in the studied climate.

Keywords: Photovoltaic, Photovoltaic/thermal, Solar collectors, Heating energy, Seasonal thermal energy storage, Air source heat pump

Introduction

Solar energy application in buildings is expected to play a major part in the global effort of carbon reduction considering that the global building sector accounted for 36% of energy consumption and 37% of CO_2 emissions in 2020 (IEA 2021). According to the reports of International Energy Agency, the global dwellings using solar thermal technologies for water heating have reached 250 million by 2020, and the electricity generated by solar PV panels exceeded 1000 TWh (1 TWh = 1 billion kWh) in 2021. In the Net Zero Emissions by 2050 Scenario, however, 290 million new solar thermal systems (IEA 2022b) and an average annual PV generation growth of 25% are needed in the years to 2030 (IEA 2022a). China has been dominating the global solar energy market thanks to the strong support from the government (Shen et al. 2021). Since 2009, the Chinese government has initiated a series of policies including project and city-scale demonstrations with subsidies (He et al. 2015) and multi-tiered feed-in tariff systems (Zhang and He 2013). Now, as the PV market has reached a grid-parity by 2022, a more complicated policy instrument is needed (Zhang et al. 2022a, b). In the solar thermal market,

Springer

Liu *et al. City and Built Environment*   (2023) 1:16

Page 2 of 21

domestic solar water heating (SWH) systems have long been popular in rural areas (Hou et al. 2022) while installations in urban areas have gained considerable increase only recently and have expanded into the space heating market (Sovacool and Martiskainen 2020). With the new carbon goal of China reaching peak emissions by 2030 and neutralization by 2060 (Zhang et al. 2022a, b), the market is seeing a growing interest in zero-carbon buildings that use a larger share of renewable energy, especially the building-integrated solar energy(Ma et al. 2021; Yu et al. 2022).

In solar planning for building energy systems, either solar photovoltaic (PV) or solar thermal collectors (STC) can be considered. One primary issue associated with solar energy is the need of energy storage to cope with its unstable nature and seasonal cycles that mismatch the demand cycle. The PV systems can be installed as off-grid systems (standalone) with batteries or on-grid systems that use the power grid as the storage media. In addition to roof-top installations, PV panels are integrated with various building components, such as windows or facades (Kuhn et al. 2021), roof tiles (Martín-Chivelet et al. 2022), awnings, and parking structures (Deshmukh and Pearce 2021) to increase installation areas. In the solar thermal utilization, the STC systems are often combined with other technologies, such as air source heat pump (ASHP) and seasonal thermal energy storage (STES) (Bie et al. 2020; Kamel et al. 2015). The heat pump has long been considered as an energy efficient and mature technology (Sadeghi et al. 2022). However, in some climates, the ASHP system is associated with declined efficiency and reduced heating capacity because of frosting issues (Qu et al. 2017). Solar-assisted heat pump (SAHP) systems, which combine solar energy and heat pump, can achieve higher efficiencies than the two systems acting alone(Fan et al. 2021; Lerch et al. 2015; Lu et al. 2021). The STES addresses seasonal imbalances of solar energy by saving excessive solar heat in the non-heating seasons for use in the heating season (Ucar and Inalli 2008). The use of thermal storage in general increases the efficiency of collectors (Kalogirou et al. 2016; Mahon et al. 2020). According to Lu et al.(2020), STES can increase the energy production of collectors from 51 to 229 kWh/m^2 in Hangzhou, China.

Solar energy is a low-density energy source. Solar energy systems normally require a large installation area to cover energy needs, which can be a challenge in buildings. Therefore, in the solar energy planning of a building, it is important to identify the system with the highest energy production rate per unit installation area. To meet the heating demand, both solar collectors and PV panels (with ASHP) can be installed. A circulating SWH system typically has an efficiency from 30 to 40% depending on solar radiation, water temperature, and ambient temperature (Gao et al. 2020; Sabiha et al. 2015). A PV + ASHP system can generate heating energy at a similar efficiency considering a typical efficiency of 13% to 20% for the PV system and a COP of 2 to 3 for the ASHP (Pedraza 2022). Recently, the development of photovoltaic/thermal (PV/T) technologies makes it possible to deliver both electricity and heating energy in a more spatially efficient way (Joshi and Dhoble 2018; Leonforte et al. 2022).

So far, there have been very few studies on comparing the energy performance of solar collectors and PV panels in terms of spatial efficiency. This study attempts to fill the gap. The energy production rates of the two solar technologies are compared through five optimized systems that use ASHP and STES in varied ways. The objective is to find out the most spatially efficient system in terms of energy production per unit of installation

area and assess its economic performance and environmental impact. The study helps the decision process in choosing proper solar technologies within the limit of installation areas.

Systems and modelling

To compare the energy capacity of various solar energy systems, the reference energy demands of domestic hot water (DHW), heating, and cooling of a residential building is chosen. In this section, a brief description of the building is presented first with prescribed heating, cooling, and DHW demands. Then various solar energy systems, along with their modelling in TRNSYS (S.A. Klein 2016), are proposed to meet the energy demands. In all systems, the DHW tank and heating terminals are not included and therefore their impact on the energy efficiency and cost is not considered. In addition, water is used as working fluid in thermal collectors for simplicity.

The site and loads

The energy demands were estimated based on a two-story house model with 220 m^2 floor area as described in (Hong et al. 2019). The building is assumed to be in Hangzhou city (30ºE, 120ºN), which is in the hot summer and cold winter region in China. The average total horizontal solar irradiation is 4,402 MJ/(m^2·yr) (Huang et al. 2014). The annual cooling and heating loads have been estimated using EnergyPlus. However, some adjustments have to be made in this study. The original building model included a solar chimney that could provide extra solar heating during the heating season. However, this is not a general feature in practice. In addition, the original model had insulation exceeding the current building codes, which is also not universal in China. For these two reasons, the heating load is increased to a more practical level. The resulting annual heating and cooling loads are 8,072 kWh and 10,709 kWh, respectively.

The domestic hot water (DHW) load was calculated based on five occupants and a daily demand of 60 °C, 40 L/person according to the national standard (MOHURD 2019).

$$Q_{DHW} = Cm(60 - t_{in}) \tag{1}$$

where Q_{DHW} is the daily DHW load (kWh/d), C is the specific heat capacity of water (kJ/kg·K), m is the daily hot water mass ($= 200$ kg/d), and t_{in} is the tap water temperature (ºC). The tap water temperature was estimated based on the measured temperature in Lake Taihu (Zheng et al. 2021), which is one of the city's supply water source. The calculated DHW load is 3,578 kWh/y.

Figure 1 plots the daily horizontal total solar radiation per unit area along with daily loads for DHW, space heating, and space cooling throughout the year. In meeting these demands, five different combinations of PV, ASHP, STC, PV/T, and STES are compared.

System A: PV with ASHP

This system consists of solar PV panels and two ASHP systems. As shown in Fig. 2, one ASHP (Type 941) is used to provide heating energy (DHW and space heating). The other ASHP (Type 655) provides cooling energy in summer. Although one single ASHP system with heat recovery could provide both chilled water for cooling and hot water for
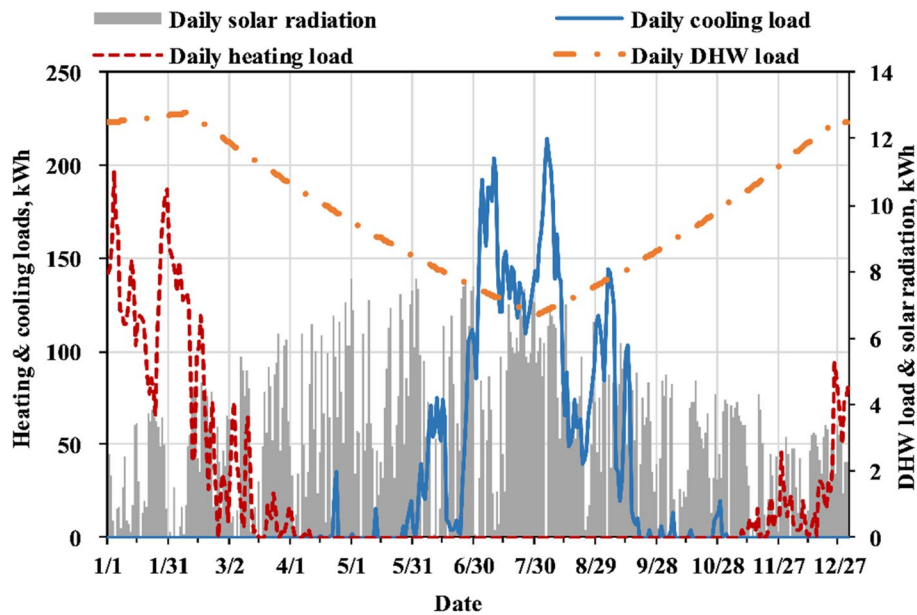
Fig. 1 Daily horizontal total solar radiation per square meter and loads of DHW, cooling, and heating throughout the year
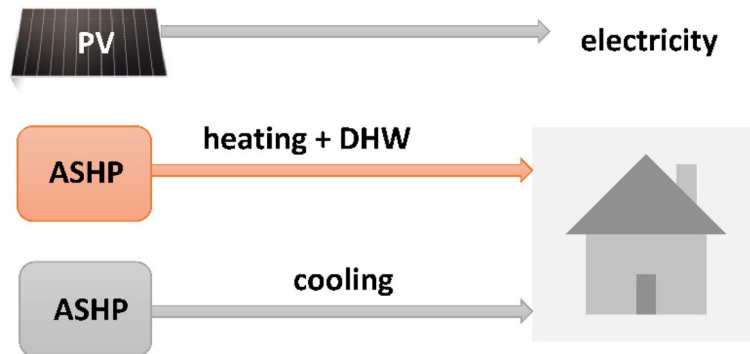

Fig. 2 PV + ASHP system

heating in summer, this is not considered in this study. The PV panel system provides all the electricity demand of the energy system.

System B: PV with ASHP assisted by STC

Compared with the system A, a solar collector system is added to provide part of the heating energy (Fig. 3). The addition of the collectors reduces the required area of PV panels because the electricity consumption of the ASHP is reduced. If the STC is more efficient than the PV panels, the overall installation area will be reduced. In Fig. 3, the STC (a flat plate collector, Type 1b) works with a small water tank (Type 4c). The STC starts to charge the water tank when its outlet temperature exceeds the bottom temperature of the tank by 10 °C and stops when the difference is below 2 °C. In addition, for safety purpose, the charging stops when the top node temperature of the tank exceeds 95 °C. The operation control puts the priority on using solar
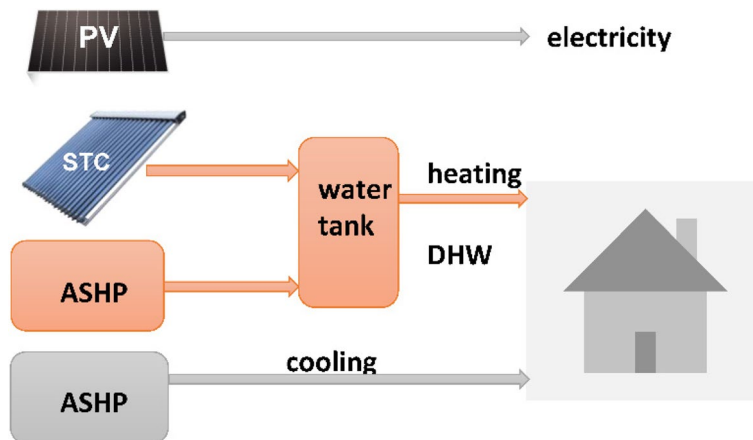
Liu *et al. City and Built Environment*   (2023) 1:16

Page 5 of 21

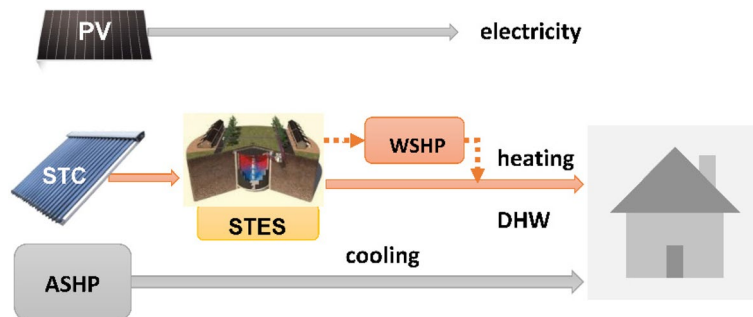**Fig. 3** PV + ASHP + STC system

Fig. 4 PV + STC + STES system

energy. The ASHP is switched on only when the tank temperature is below 40 °C and is switched off once the temperature is above 45 °C.

System C: PV with STC and STES

Compared with system B, system C uses the STC and STES to provide the heating energy and the ASHP is only used for cooling purpose (Fig. 4). The STES (a buried type, Type 4c) has an initial temperature of 45 °C and is modelled as a stratified water tank that loses heat to the surrounding soil of 16 °C at a rate of 0.1 W/(m^2·K). To ensure that no pre-stored energy in the tank is used in a one-year cycle, the system is sized such that the year-end temperature of the tank is no less than its initial temperature (45 °C). In this way, the system is sustainable with 100% of the heating energy coming from the solar energy of the current year, not partially from previous years. This is true for all cases with the STES.

A water-source heat pump (WSHP, Type 927) is used to raise the water temperature for heating when the tank temperature falls below 45 °C. To prevent the formation of ice or too low COPs, tank temperatures below 8 °C shall be avoided.
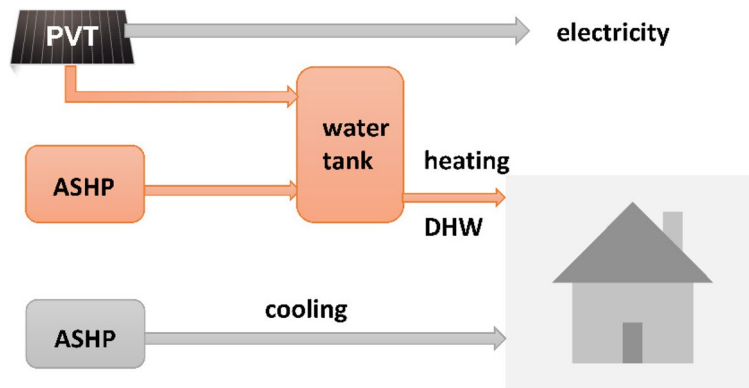
Liu *et al. City and Built Environment*　　(2023) 1:16

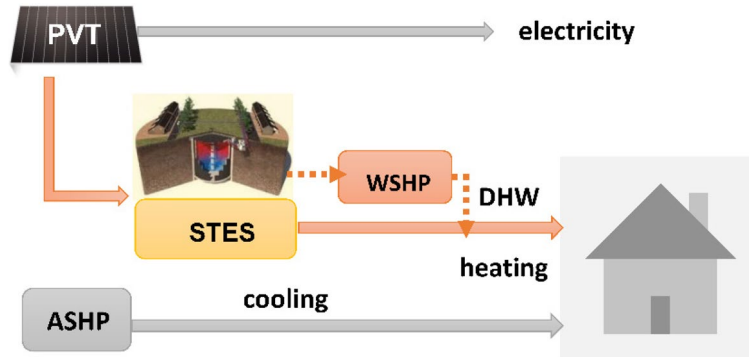Page 6 of 21

Fig. 5 PV/T + ASHP system

Fig. 6 PV/T + STES system

System D: PV/T with ASHP

Compared with system B, system D replaces the STC with the PV/T (Type 50a) panels (Fig. 5). The heat transfer fluid in the PVT system is water because the freezing issue is not a concern in this study region. The thermal efficiency of PV/T panels is generally lower than the STC. Like in system B, the collected solar energy is also used first before the ASHP, i.e., the ASHP only works when the tank temperature drops below 40 °C and stops once the temperature of the tank is above 45 °C again. The optimized system sizes are such that the annual electricity production of the PV/T balances the total electricity demand by the ASHPs.

System E: PV/T with STES

System E relates to system D in the same way that system C relates to system B (Fig. 6). A seasonal storage tank is added to test its impact on the system efficiency. Like in system C, the initial temperature of the tank is set to 45 °C and the system is sized such that the year-end temperature of the tank is no less than its initial temperature (45 °C).

Liu *et al. City and Built Environment*   (2023) 1:16

Page 7 of 21

Table 1 System parameters used in TRNSYS modelling

Model	Parameter	Value
Solar collectors	Intercept efficiency	0.8
(Type 1b)	Efficiency slope, kJ/(h·m^2·K)	13
	Efficiency curvature, kJ/(h·m^2·K^2)	0.05
	Installation slope, degree	30
	Azimuth angle (From true north), degree	180
ASHP for heating	Rated heating capacity, kW	11.24
(Type 941)	Rated heating power, kW	3.26
ASHP for cooling	Rated heating capacity, kW	11.64
(Type 655)	Rated COP	3
Pump	Solar pump flow rate, kg/h	variable
(Type 3b)	ASHP pump flow rate, kg/h	900
	Load side pump flow rate, kg/h	800
WHSP	Heating loop pump flow rate, kg/h	900
(Type 927)	Rated heating capacity, kW	11
	Rated heating power, kW	1.9
Storage tank	Average tank loss coefficient, W/(m^2·K)	0.33
(Type 4c)	Initial storage temperature in all layers, ℃	40
	Ambient temperature, ℃	22
	Number of tank nodes	5
Seasonal tank	Average tank loss coefficient, W/(m^2·K)	0.1
(Type 4c)	Initial storage temperature in all layers, ℃	45
	Soil temperature, ℃	16
PV	Module area, m^2	1.717
(Type 94a)	Module short-circuit current at reference conditions, A	8.98
	Module open-circuit voltage at reference conditions, V	38.39
	Module voltage at max power point and reference conditions, V	30.94
	Module current at max power point and reference conditions, A	8.56
	Temperature coefficient of I_{sc} at reference condition	0.067
	Temperature coefficient of V_{oc} at reference condition	-0.33
	Installation slope, degree	30
	Azimuth angle (from true north), degree	180
PV/T	Cell efficiency	0.17
(Type 50a)	Collector plate absorptance	0.92
	Collector loss coefficient, kJ/(h·m^2·K)	16
	Cover transmittance	0.89
	Packing factor	0.8
	Installation slope, degree	30
	Azimuth angle (from true north), degree	180
Users loads	Total heating loads, kWh	11,650
(Type 682)	Total cooling loads, kWh	10,709

System input parameters and optimization

The modelling and simulation of the above five systems were performed in TRNSYS. Table 1 presents the system parameters and initial conditions. The ASHP and WSHP were rated to meet the maximum hourly heating and cooling loads, respectively. The circulation pumps were rated to deliver the heat to meet the maximum hourly loads at a temperature difference ranging from 5 to 10 °C. The rated COPs of ASHP and
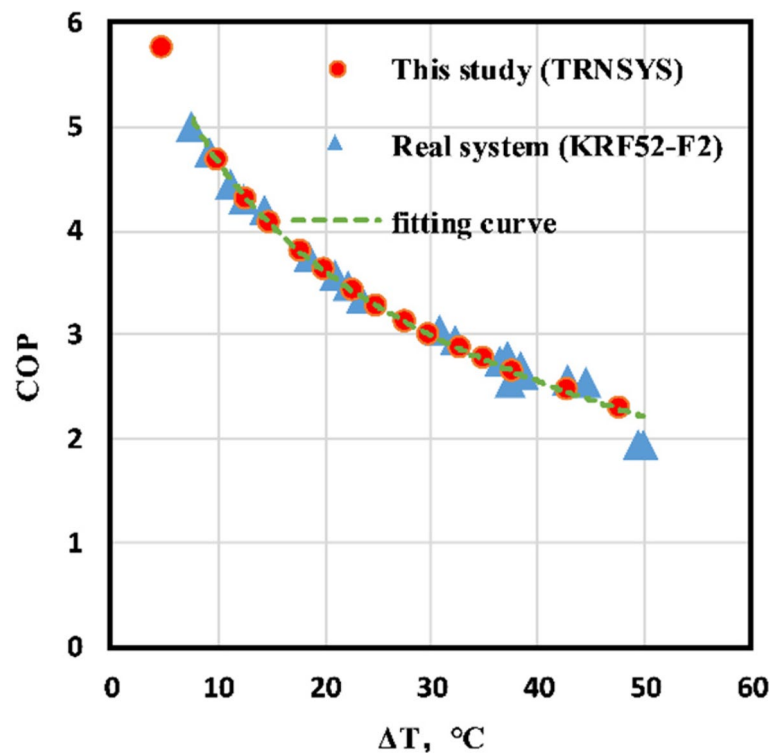
Fig. 7 The COP curve of the chosen ASHP in TRNSYS and its comparison with a real system (5.2 kW, Guo et al. 2019)

WSHP were in accordance with the national standards (Standardization administration 2015). For the ASHP, the rated heating capacity was 11.24 kW and its COP curve was set in TRNSYS to match the measured data from a unit of similar size, as shown in Fig. 7.

The electricity production of the PV panels was estimated in TRNSYS based on parameters in Table 1 and the Typical Metrological Year data of Hangzhou (China Meteorological Administration and Tsinghua University 2005). The resulted annual production rate was 192.45 kWh/m^2. Using a decline rate of 2.5% for the first year and 0.7% for the 19 years after (China Electricity Council 2021), an average rate of 177.08 kWh/m^2, or 14.1% in terms of electricity production efficiency, was obtained for a 20-year life cycle. This average rate was used to calculate the area of PV panels needed to balance all power consumptions in each system. All systems consider an on-grid PV system so that no electricity is wasted because of mismatches between loads and production.

The PV/T was modelled in TRNSYS with a constant loss coefficient. The packing factor, which is the ratio of the PV cell area to the absorber area, is 80%. The following default collector efficiency in TRNSYS (S.A. Klein 2016) was used:

$$\eta = 0.786 - 15.36 \frac{(t - t_a)}{G} \tag{2}$$

where t is the collector temperature (ºC), t_a is the ambient temperature (ºC), and G is the solar radiation (kJ/h·m^2).

The simulation involved optimization to find the minimal size for a given system to meet the energy demand. For system A, minimal tank volumes for different ASHP heating capacities were searched. For systems C and E, minimal sizes of the STES for different collector areas were searched. The heating demand was considered met when the difference between the supplied heat and the heating load was less than 1% of the heating load for every hour. Rarely, the 1% criterion was exceeded. When this occurred, the simulation was still considered valid if the water supply temperatures at these hours were higher than 40 ℃. There was still heating capacity for water above this temperature.

The heat loss of piping work was neglected. The flow rate of the solar pump was estimated based on a ratio of 0.063 m³/h per square meter of collector area (MOHURD 2018).

Performance indexes

The thermal efficiency of solar systems is defined as the total delivered heating energy divided by the total received solar irradiation on the solar panels (e.g. thermal collector or PVT):

$$\eta_1 = \frac{Q}{\Phi} \tag{3}$$

where η_1 is the thermal efficiency, Q (kWh) is the heating energy output, and Φ (kWh) is the total received solar radiation. This efficiency differs from the collector efficiency (see Eq. 2) in that the system efficiency is concerned with the heating energy delivered to the heating loop while the collector efficiency is only concerned with the energy delivered to the storage tank. For systems without storage tank, the two efficiencies are the same.

The electricity production efficiency of PV or PVT panels is defined as:

$$\eta_2 = \frac{W}{\Phi} \tag{4}$$

where η_2 is the electricity production efficiency and W (kWh) is the total electricity generated. When the generated electricity is used to drive the ASHP to deliver heating energy, the thermal efficiency can be calculated using Eq. (3), where the heating energy output is the heat energy delivered by the heat pump.

The spatial efficiency of solar systems is evaluated as the total installation area per unit of energy demands. Alternatively, it can be substituted by the energy capacity of systems, which is defined as the total energy delivered per installation area:

$$\varepsilon = \frac{\text{Total energy output}}{A_{TOT}} \tag{5}$$

where ε (kWh/m²) is the energy capacity of the system. The total installation area is the sum of the required areas for the PV panels, PV/T panels, and STCs:

$$A_{TOT} = \sum_i A_i \tag{6}$$

$$A_{PV} = \text{MAX}\left(\frac{E}{p}, 0\right) \tag{7}$$

where A_{TOT} (m^2) is the total installation area, A_i (m^2) is the area of solar panels (i = PV, PV/T, or STC). E is the total electricity consumption (kWh/y), and p is the electricity production rate of PV panels (= 177.08 kWh/(m^2·y)). The heat pump units and STES can be placed in shaded areas and are not necessarily competing against solar panels. Therefore, the spaces for these components are not considered. E is negative if the system produces more electricity than it consumes. The heating and DHW demands are met using water supplied at temperatures of 45 °C.

The economic performance is evaluated using the equivalent annual cost (EAC), which is the annual cost in the whole life cycle of the system considering the initial investment, operation and maintenance (Vijay and Hawkes 2019).

$$\text{EAC} = C\frac{r(r+1)^n}{(r+1)^n - 1} + P_E \cdot E + \alpha C \tag{8}$$

where C (CNY) is the initial investment, r is the discount rate (= 8%), n is the lifetime of the system (= 20 years), P_E is the local utility price (a tiered pricing: 0.536 CNY/kWh up to 2760 kWh, 0.588 CNY/kWh for between 2760 and 4800 kWh, and 0.838 CNY/kWh for > 4800 kWh). α is the ratio of the annual maintenance cost to the initial investment (= 1%). The initial investment is estimated using Eq. (7).

$$C = \sum_i c_i \cdot A_i + \sum_j C_j + c_{STES} \cdot V_{STES} + C_{p\&p} \tag{9}$$

where c_i (CNY/m^2) is the unit cost (i = PV, PV/T, or STC), C_j (CNY) is the component cost (j = ASHP or WSHP). c_{STES} (CNY/m^3) is the unit cost of the tank and V_{STES} is the tank volume. $C_{p\&p}$ is the cost of pumps and pipe working. Table 2 gives the prices of the components used.

The environmental impact is evaluated using the carbon emission of the system in a life cycle. This includes the embodied carbon emissions and the emissions during the operation phase as shown in Eq. (10).

$$CE = \sum_i ce_i \cdot A_i + \sum_j CE_j \frac{20}{LT_j} + \epsilon \cdot E \tag{10}$$

where CE (kg CO$_2$ eq.) is the total emission in a life cycle, ce_i is the embodied emission per unit area of the solar panel i, CE_j is the embodied emission for the component j (j = ASHP, WSHP, and STES), LT_j (y) is the lifetime, and ϵ is the carbon emission factor of power grid. Table 3 lists the emission factors for the three types of solar panels. The embodied carbon emission for ASHP and STES tanks were estimated based on materials

Table 2 Component prices used in cost evaluation

Parameter	c_i (CNY/m^2)			C_j (CNY)		$C_{p\&p}$ (CNY)	c_{STES} (CNY)	
Description	PV/T	PV	STC	ASHP	WSHP	Pumps & Piping	Buried tank	Surface
Value	1948	1345	1000	35,000	10,000	3000	1867	1100
Reference	(Sifnaios et al. 2021)	(Lu et al. 2020)					(Chu et al. 2022)	

Exchange rate between Chinese yuan and US dollar: CNY: USD = 6.72:1 (China State Administration of Foreign Exchange 2023)

Table 3 Parameters used in carbon emission evaluation

Parameter	ce_i, kg CO_2 eq./m^2			CE_j, kg CO_2 eq./unit			ϵ, kg CO_2 eq./kWh
Description	PV	PV/T	STC	ASHP	WSHP	STES	
Value	293.24	387.00	231.02	5254	3284	519.31 $\times V_{STES}$+ 771.64 for small tanks 296.1 $\times V_{STES}$ +16404 for buried tanks	0.5810
Reference	(Li et al. 2022)	(Good 2016)	(Li et al. 2022)	(Yang et al. 2018)	-	-	(China Ministry of Ecology and Environment 2022)

Table 4 Simulation results for the PV + ASHP heating systems with different rated capacity

Percentage of fully rated P_{hp}	Min. tank volume (m^3)	Tank heat loss (kWh)	Power consumption for heating (kWh)	ASHP COP
100%*P_{hp}	3.3	835	4895	2.82
90%*P_{hp}	4.5	1000	4865	2.86
80%*P_{hp}	12.1	1933	5133	2.90
70%*P_{hp}	55.5	6093	6431	3.00

and its carbon emission factors (Yuancheng and Bin 2018). The *CE* for WSHP was estimated as 0.625 times of the ASHP of similar heating capacity (Greening and Azapagic 2012). Two correlations were obtained for the tanks because the insulation was different: the insulation is 0.1 m polyurethane for small tanks and 0.2 m for buried tanks. The lifetime is assumed to be the same as that of the system ($LT_j = n$) for all components and solar panels.

Results

System A: PV with ASHP

The ASHP heating system typically works with a buffering tank, which helps reduce partial load losses associated with the heat pump not working at its full capacity (Conti et al. 2022). The disadvantage is that the tank also introduces heat losses. The partial load, however, is not considered in the present study.

The use of a tank allows a reduced size of ASHP. The larger the tank is, the smaller the size of the ASHP can be. Table 4 shows the energy simulation results for the ASHP at different rated heating capacities. The size of the ASHP has little impact on the total power consumption when the tank volume is less than 12 m^3. System A consumes approximately 4900 kWh in total for heating, which can be met with 35.5 m^2 of PV panels. However, the heat loss of the tank increases considerably as the size increases. In the case of 70% rating, the tank needs to be at least 55.5 tons, and almost 1/3 of the generated heat is lost by the tank. The loss increases the total power consumption. Therefore, a large tank should be avoided for the ASHP system. Note that the overall COP value of the ASHP ranges from 2.82 to 3.00.

System B: PV with ASHP assisted by STC

Table 5 shows the changes in energy performance of the system when different areas of STC are added. The first row is System A with 35.5 m^2 of PV panels. Introducing collectors into the system reduces the need for PV panels. The difference between the reduced PV area and the collector area is the reduced installation area. Maximum reduction occurs at STC = 3 m^2. However, the reduced installation area is negligible. The reduction diminishes after STC = 5 m^2. At somewhere between STC = 3 m^2 and 5 m^2, the thermal collectors and the PV panels share the same annual thermal efficiency. From Table 5, it can be seen the collector efficiency at this point is between 43.7% and 46.5%. The thermal efficiency is lower due to the thermal loss. Nonetheless, it should be very close to the thermal efficiency of PV + ASHP (43%), which can be estimated as the product of the electricity production efficiency (15.3% for the first year, see Sect. "System input parameters and optimization") and the average COP of the ASHP (2.82, see Table 4). In other words, in order for collectors to be as thermally efficient as the PV panels in delivering heating energy, its annual collector efficiency needs to reach at least 43%. In real applications, it is difficult for a system with a large size of collectors to achieve this threshold without thermal storage because a large portion of solar energy cannot be utilized in summer as a result of seasonal mismatches between solar energy and building loads.

System C: PV with STC and STES

In system C, various combinations of three parameters were simulated: the STC area, the tank volume, and the use of WSHP. Figure 8 shows the influences of the three parameters on the energy performance. Some combinations fail to meet the heating demand with an ending tank temperature below the initial temperature of the storage tank (45 ℃), which is not sustainable. These failed cases are plotted in hollow symbols (circles). Points of solid symbols represent cases where the heating demand is met. All cases with $A_{STC} = 40$ m^2 fail except for the first point (tank = 80 m^3).

For each collector area, there exists an optimal tank volume that corresponds to the minimal power consumption. Large tanks have greater heat losses, which may make the system unable to meet the heating demand. For example, the system with $A_{STC} = 44$ m^2 fails to meet the heating demand when the tank size is greater than 220 m^3 (hollow symbols). The electricity consumption by the WSHP is also shown in Fig. 8 for the $A_{STC} = 55$

Table 5 Performance results with different collector areas added

Collector area (m^2)	Collector efficiency	Power consumption for heating (kWh)	Reduced PV area (m^2) [a]	Reduced installation area (m^2)
0	0.0%	4895	0.0	0.00
1	47.0%	4713	1.03	0.03
3	46.5%	4356	3.04	0.04
5	43.7%	4069	4.66	-0.34
7	40.4%	3844	5.94	-1.06
10	34.9%	3629	7.15	-2.85
20	25.0%	3203	9.56	-10.44
40	15.4%	2630	12.79	-27.21

[a] The reduced PV area for each collector area is calculated based on a PV production rate of 177.08 kWh/m^2

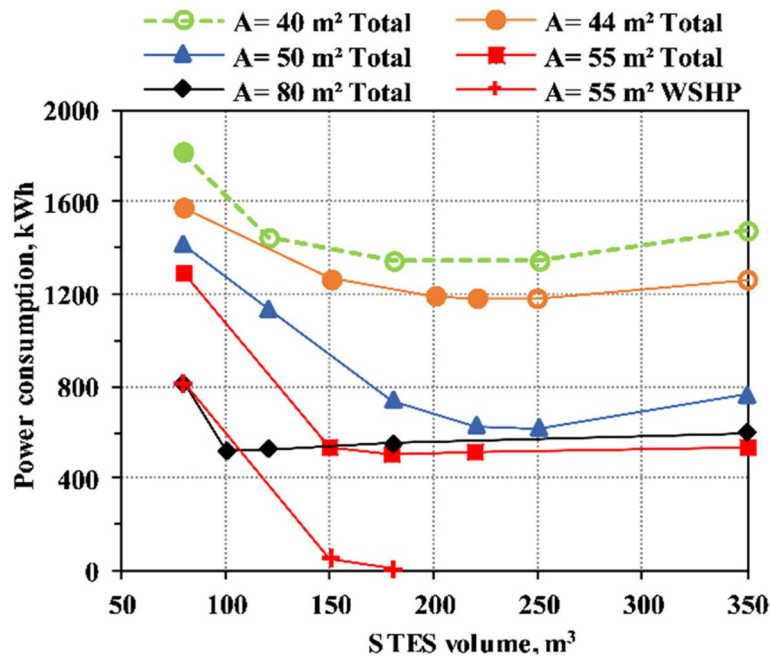Liu *et al. City and Built Environment*   (2023) 1:16

Page 13 of 21

Fig. 8 The variations of total power consumption and WSHP consumption with STES tank volume at different collector areas
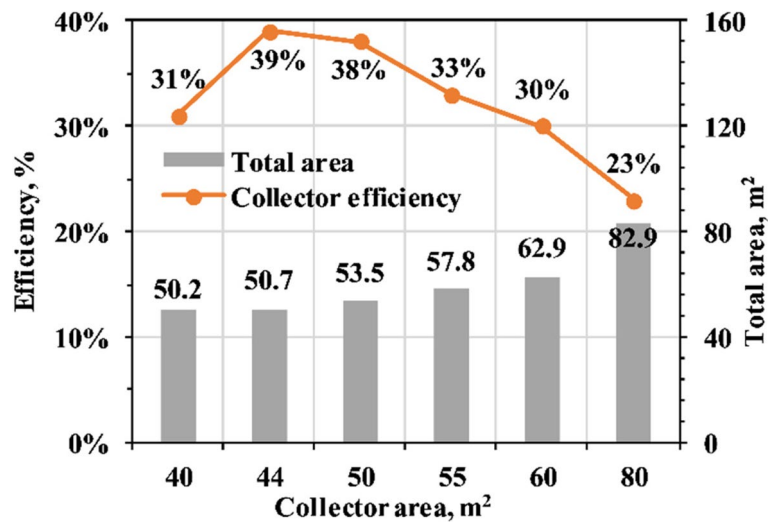

Fig. 9 The total installation areas, STES volumes, and collector efficiencies at different collector areas

m^2 case. The minimal energy consumption is shown to occur at zero WSHP energy. This implies that the WSHP does not necessarily increase efficiency, but it helps reduce the tank volume.

When the PV panels are used to balance the electricity consumption by the circulation pump and the WSHP, the total installation area (STC + PV panels, heating only) for each collector area can be obtained and is plotted in Fig. 9 along with the collector efficiency. The smallest total installation area (50.2 m^2) occurs at the smallest collector size:

$A_{STC} = 40$ m^2. Although a smaller total installation area appears available with smaller sizes of collectors, the difference would be minimal. From Fig. 9, it is also evident that the use of STES increases the thermal efficiency of the collectors. For an example, at $A_{STC} = 40$ m^2, the collector efficiency (31%) doubles compared with that of the case without the STES (15.4%, in Table 5).

System D: PV/T with ASHP

Compared with system B, system D replaces STC with PV/T. Figure 10 plots the thermal efficiency of the PV/T and the total installation area (PV/T + PV) at various PV/T areas. Again, the PV panels are to balance any remaining electricity. Like system B, the thermal efficiency of PV/T declines as the PV/T area increases. The least installation area (23.2 m^2: PVT = 10 m^2, PV = 13.2 m^2) is 4.3 m^2 less than the minimal installation area of systems A and B. Further increasing the PVT areas results in surplus electricity production and wasted thermal energy.

The thermal efficiency of the PV/T is generally lower than that of the STC. However, when the area is greater than 12 m^2, their differences become small. The threshold thermal efficiency of PV/T will be much smaller than that of STC because the PV/T produces electricity as well.

System E: PV/T with STES

In this system, an STES tank is used to improve the thermal efficiency of the PV/T. Figure 11 shows the simulation results with varied PV/T areas and STES sizes. The hollow symbols indicate that the system is unable to meet the heating demand without using the pre-stored energy in the storage tank. Again, compared with system D, system E achieves higher thermal collection efficiency at large collector areas thanks to the use of STES. For instance, at $A_{PVT} = 50$ m^2, the thermal efficiency of system E (31.7%) is almost
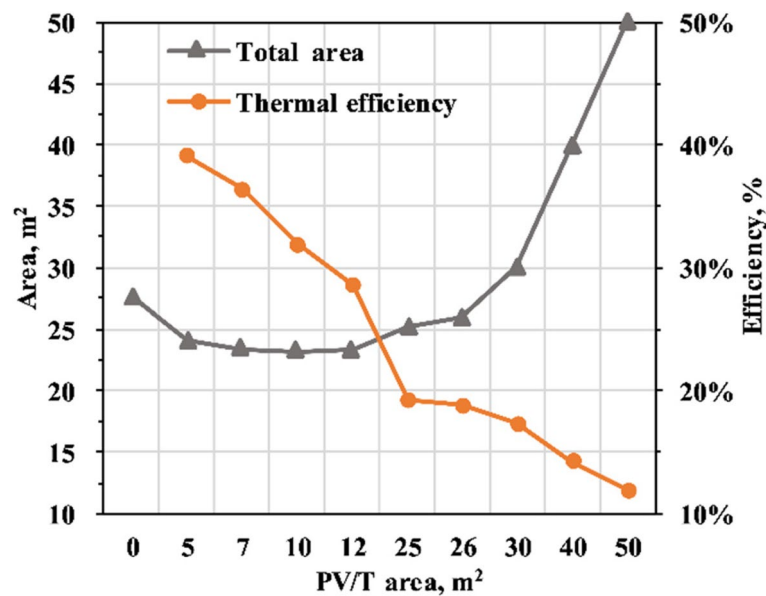

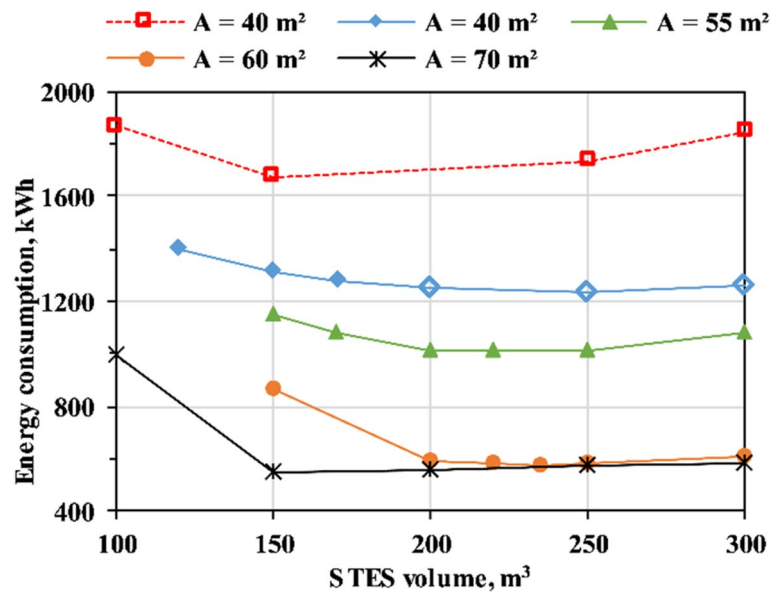**Fig. 10** Performance operating conditions by increasing the PV/T areas

Fig. 11 Power consumptions vs. STES volumes at varied PV/T panel areas

triple of system D (11.9%). In addition, the electrical efficiency of system E (10.7%) is also higher than that of system D (9.4%). This is because the use of STES allows the PV/T to operate at lower temperatures. However, this system requires greater installation area (50 m² of PV/T). The reason is obvious: The STES tank introduces considerable thermal losses. Note that there is surplus electricity. With 50 m² of PV/T, the electricity production is 6696 kWh for the first year. Assuming a first-year decline rate of 2.5% and 0.7% thereafter, the average electricity production for a 20-year life cycle is 6161 kWh/y and the average surplus electricity is 1,801 kWh/y. The surplus electricity is not accounted for in the area comparison, but it will affect the cost and environmental impact assessment.

Area comparison

In this section, the total installation areas (solar panels for heating and cooling) are compared. The cooling of the building was simulated separately with the supplied chilled water temperature between 7 and 12 °C. The simulation resulted in an amount of electrical consumption of 3079 kWh for the total annual cooling load of 10,709 kWh. In all cases, the PV system is used to balance any remaining electricity balance after the electricity produced by the PV/T, if present, is accounted for.

The minimum total installation area of each system is shown in Fig. 12. The benchmark system (the PV + ASHP system, or system A) requires an installation area of 44.9 m² (PV panels). Introducing a proper size of STC (system B) can only reduce the installation area by less than 0.1 m². Introducing STES (system C) does not reduce the total installation area. Instead, this system requires the most installation area. However, introducing PV/T (system D) is advantageous with a least total area of 40.6 m², a reduction of 4.3 m² compared with the benchmark case. Preferably, PV/T is used without the STES.

The values of energy capacity for systems A, B, C, D, and E are 498 kWh/m², 497 kWh/m², 331 kWh/m², 551 kWh/m², and 494 kWh/m², respectively. If only the heating system
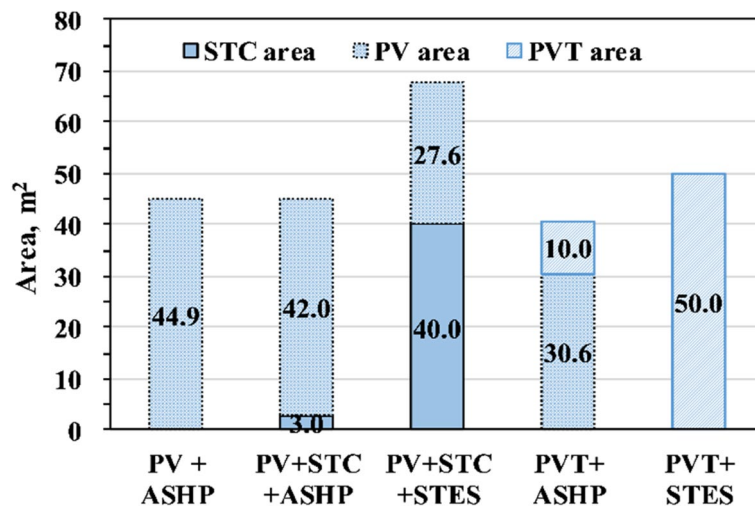
Fig. 12 The minimum total installation areas for the five systems

Table 6 The initial cost, EAC, and carbon emission of five systems and the conventional system

System: descriptions	Initial Cost (CNY)	EAC (CNY/y)	Total embodied carbon (kgCO$_2$ eq.)	Total carbon emission (kgCO$_2$ eq.)
A: PV + ASHP + ASHP	138,288	15,468	26,772	26,772
B: PV + STC + ASHP + ASHP	136,102	15,223	25,999	25,999
C: PV + STC + STES + WSHP + ASHP	261,123	29,207	60,871	60,871
D: PVT + ASHP + ASHP	137,224	15,349	25,827	25,827
E: PVT + WSHP + STES + ASHP	472,790	51,917	94,629	73,698
Conventional systems: ASHP + ASHP	77,950	14,752	13,617	96,728

Currency exchange rate: CNY: USD = 6.72:1 (China State Administration of Foreign Exchange 2023)

is considered, the energy capacities for these systems in the same order are 424 kWh/m^2, 422 kWh/m^2, 232 kWh/m^2, 503 kWh/m^2, and 523 kWh/m^2, respectively. The values for heating systems only are generally lower than those for cooling and heating systems together because apparently the cooling system is more energy efficient than the heating system. System E appears to be an exception because the surplus electricity generation is not counted in the heating cycle.

Cost and environment impact

Table 6 compares the economic performance and environmental impact of the five systems, each in its minimal installation area, in a 20-year lifetime. System B turns out to be the most economical system. However, the other two systems (A and D) are only slightly higher. The systems with STES (C and E) cost 1.9 to 3.4 times of the other three systems without STES. The main reason is that the STES with a water tank is not an economical technology (Lu et al. 2020). The comparison result is not sensitive to the utility price because only system E has surplus electricity, and the amount is not influential. The last row of the table is the conventional system which is the same as system A except that the

PV is removed, and all power is from the grid. In comparison, system B costs only 3.2% more than the conventional system.

System D emits the least carbon in its 20-year lifetime, but its advantage over systems A and B is small. The systems with STES (C and E) have much greater impact than the other three systems without STES. System E emits the most carbon dioxide. Its impact is 2.85 times of that of system D. The higher emission is due to the large STES tank. Nevertheless, all five solar systems have less environmental impact than the conventional system. Among them, systems A, B, D can reduce the impact by 72% in a lifetime of 20 years.

Discussions

From Sect. "Area comparison", it is found that systems A and B share similar energy capacities. However, a closer examination of the optimization of system B reveals that the thermal collector in a large area is less efficient than the PV. In the studied climate, the equivalent thermal efficiency of the PV panel (with ASHP) is approximately 43%. Although the instantaneous thermal collector efficiency can be greater than this value, the annual average is much smaller because the mismatches between loads and solar energy reduces the portion of collected energy to be unutilized. The PV system does not have such losses if it can use the power grid as the storage. What is surprising is that even the STES cannot change to favour the solar collectors. Although the STES can increase the efficiency of the STC considerably, its thermal losses still prevent the STC from matching up with the PV panel in energy capacity.

Integrating PV with thermal collectors can help reduce the installation area. Among the five studied systems, system D uses the smallest area indicating that PV/T is the most spatially efficient panels. In the studied climate, PV/T system can deliver 551 kWh/m^2 of energy (cooling + heating), 10.6% higher than the PV system (with ASHP).

As previously mentioned, solar energy is an important source for fighting global warming. Our results show that adding solar energy systems can achieve 72% of emission reduction compared with the conventional ASHP heating system that uses grid power. Therefore, promoting solar panels in buildings is an effective solution to fight the global warming considering the large building stock.

Solar systems are not yet cost effective compared with the conventional ASHP heating system that uses grid power. Regardless of the forms of solar panels, the addition of solar energy systems increases the EAC value by 3.2% (Sect. "Cost and environment impact"). An earlier study (Lu et al. 2020) has shown that solar heating systems using STC have no economic advantages over the conventional ASHP heating systems. Here it is further shown that not only STC but also PV and PV/T have no economic advantages over the ASHP heating systems. But this could change if the utility price becomes higher. Further calculation shows that at a fixed utility price of 0.7 CNY/kWh, the EAC of the solar energy systems would be the same as the conventional ASHP heating system. This means that if the solar energy system is to have a realistic payback period, the utility price should be greater than 0.7 CNY/kWh.

The EAC values of the three systems (A, B, and D) are very close, indicating that PV, STC, and PVT do not pose significant economic advantages over each other. However, STES adds to the cost considerably. Current STES using water tanks is neither

cost-effective nor environmentally friendly. It presents two obvious issues. Firstly, it is associated with high thermal loss ratios. In previous simulations, the STES tank has a thermal loss rate of 0.1 W/(m²·K), which means a typically well-insulated storage tank (Del Amo et al. 2020). Even so, the thermal loss is still significant: approximately 49.2% of the energy collected is lost in system C. Various seasonal storage technologies have been developed that can keep the thermal loss to a minimum, such as thermochemical storage (Kant and Pitchumani 2022) and latent heat storage (Umair et al. 2019). These new technologies may help the STC for higher efficiency. Secondly, it has low energy density, which means that the tank often needs to be very large. Large tanks are associated with high system's EAC and high embodied carbon. For the tank to be small, STES with higher energy density is needed. There are high temperature collectors (Gaudino et al. 2022), which make it possible to have higher storage temperature and hence higher energy storage density. In addition, research is also active in searching for cost-effective STES in previously mentioned thermochemical storage and latent heat storage.

Limitations

In this study, a comparison of energy production efficiency between solar collectors and PV panels for heating and cooling is presented. The mismatches of seasonal variations between the solar radiation and the heating demand are resolved using an STES to shift the demand. An alternative to this energy shift is to use the thermal energy for cooling. Several technologies are available for that purpose, such as solar absorption cooling (Alobaid et al. 2017; Hang et al. 2013) or solar adsorption cooling (Chauhan et al. 2022). The solar thermal system generating electricity using organic Rankine cycle is also a hot topic (Sun et al. 2020). These systems typically have an overall low thermal utilization efficiency although they may increase the thermal collector efficiency (Bataineh and Alrifai 2015). Because these technologies have a low market maturity, they are not included in this study.

Furthermore, the thermal efficiency of the PV + ASHP system is highly dependent on the COP of the ASHP, which is related to the climates. The ASHP is a recognized energy efficient technology in the hot summer and cold winter region of China (Chen and Nan 2022). However, in colder climates, its efficiency will be lower (Zhang et al. 2017), which will make solar collectors more favourable. In addition, other factors may need to be considered, such as the solar radiation levels. Therefore, a specific analysis is recommended in different climates.

Conclusions

There are various options available to provide the building energy need with solar energy. Among them are the choices of solar PV panels, solar collectors, and PV/T. The study examined five solar energy systems that varied in the way of using solar energy with other technologies such as heat pump and STES to meet the heating demand (space heating and domestic hot water) for a two-story single-family house in Hangzhou, China. Cooling was considered too, but the method was the same in all cases. What is of interest is which system requires the least installation area of solar panels and what the associated cost and environmental impact are from a life cycle perspective. The conclusions are as follows:

Liu *et al. City and Built Environment*   (2023) 1:16

Page 19 of 21

1) Among the three types of solar panels (STC, PV, and PV/T), PV/T is the most spatially efficient with an energy capacity of 551 kWh/m^2 working with ASHP. The preferred heating system is PV/T with ASHP (system D), which requires the minimal installation area of 40.6 m^2 to meet the energy demand of the studied house.

2) In a larger scale, the PV system working with ASHP is more efficient than the solar thermal collector system. The thermal energy efficiency of PV + ASHP is approximately 43% in the studied climate. The annual efficiency of the STC is much lower because of the mismatches between the seasonal variations of the load and the solar energy. To exceed this value, the STC system needs to work with an efficient STES that minimizes thermal losses.

3) For the optimized systems involving the three types of solar panels, the EAC values in a 20-year life cycle are similar so long as the STES is not involved. At current tiered utility pricing in the residential sector, the addition of solar energy systems to a conventional ASHP heating system that uses grid power increases the EAC value by 3.2%. However, solar energy systems could be cost-effective when the utility price is increased above 0.7 CNY/kWh.

4) All five solar systems are effective in reducing environmental impact. In particular, the systems without STES can achieve 72% of emission reduction compared with a conventional heating system that uses ASHP only.

5) The sensible STES with water can increase the efficiency of STC. However, its thermal loss is considerable and limits the energy efficiency of STC. In addition, it usually comes with a large size because its energy density is low. This makes the current STES neither economically appealing nor environmentally friendly.

It is important to understand the role of the ASHP in the conversion of thermal efficiency of the PV panels. When the ASHP is less efficient than that in the studied climate, the PV will be less appealing compared with the STC. Therefore, the conclusion is only valid for the studied climate.

Declarations

References
Alobaid M, Hughes B, Calautit JK, O'Connor D, Heyes A (2017) A review of solar driven absorption cooling with photovoltaic thermal systems. Renew Sustain Energy Rev 76:728–742. https://doi.org/10.1016/J.RSER.2017.03.081

Bataineh KM, Alrifai S (2015) Recent trends in solar thermal sorption cooling system technology. Adv Mech Eng 7(5):1–20. https://doi.org/10.1177/1687814015586120

Bie Y, Li Z, Lei J, Ma Z, Li M, Królczyk G, Li W (2020) Solar medium-low temperature thermal utilization and effect analysis of boundary Condition: A Tutorial. Sol Energy 197:238–253. https://doi.org/10.1016/J.SOLENER.2020.01.016

Chauhan PR, Kaushik SC, Tyagi SK (2022) Current status and technological advancements in adsorption refrigeration systems: a review. Renew Sustain Energy Rev 154:111808. https://doi.org/10.1016/J.RSER.2021.111808

Chen Q, Nan L (2022) Energy, emissions, economic analysis of air-source heat pump with radiant heating system in hot-summer and cold-winter zone in China. Energy Sustain Dev 70:10–22. https://doi.org/10.1016/J.ESD.2022.07.002

China Ministry of Ecology and Environment (2022) Enterprise Greenhouse Gas Emission Accounting Methods and Reporting Guidelines Power Generation Facilities (2022 Revision). https://www.mee.gov.cn/xxgk2018/xxgk/xxgk06/202203/t20220315_971468.html

China Electricity Council (2021) Specification of Photovoltaic Power Generation Efficiency. GB/T 39857–2021

China Meteorological Administration and Tsinghua University (2005) Meteorological Data Set for China Building Thermal Environment Analysis. China Architecture and Building Press, Beijing

China State Administration of Foreign Exchange (2023) RMB against Major Foreign Currency Annual Average Exchange Rate. http://www.safe.gov.cn/safe/index.html

Chu S, Sethuvenkatraman S, Goldsworthy M, Yuan G (2022) Techno-economic assessment of solar assisted precinct level heating systems with seasonal heat storage for Australian cities. Renew Energy 201:841–853. https://doi.org/10.1016/J.RENENE.2022.11.011

Conti P, Franco A, Bartoli C, Testi D (2022) A design methodology for thermal storages in heat pump systems to reduce partial-load losses. Appl Therm Eng 215(July):118971. https://doi.org/10.1016/j.applthermaleng.2022.118971

Del Amo A, Martínez-Gracia A, Pintanel T, Bayod-Rújula A A, Torné S (2020) Analysis and Optimization of a Heat Pump System Coupled to an Installation of PVT Panels and a Seasonal Storage Tank on an Educational Building. Energy Build 226. https://doi.org/10.1016/j.enbuild.2020.110373

Deshmukh SS, Pearce JM (2021) Electric vehicle charging potential from retail parking lot solar photovoltaic awnings. Renew Energy 169:608–617. https://doi.org/10.1016/J.RENENE.2021.01.068

Fan Y, Zhao X, Han Z, Li J, Badiei A, Akhlaghi YG, Liu Z (2021) Scientific and Technological Progress and Future Perspectives of the Solar Assisted Heat Pump (SAHP) System. Energy 229(2021):120719. https://doi.org/10.1016/j.energy.2021.120719

Gao D, Gao G, Cao J, Zhong S, Ren X, Dabwan YN, Hu M et al (2020) Experimental and numerical analysis of an efficiently optimized evacuated flat plate solar collector under medium temperature. Appl Energy 269:115129. https://doi.org/10.1016/j.apenergy.2020.115129

Gaudino E, Musto M, Caldarelli A, De Luca D, Di Gennaro E, Russo R (2022) Evaluation of the absorber temperature frequency function valid for evacuated flat plate collectors. Energy Rep 8:1071–1080. https://doi.org/10.1016/J.EGYR.2022.05.275

Good C (2016) environmental impact assessments of hybrid photovoltaic-thermal (PV/T) Systems - a review. Renew Sustain Energy Rev 55:234–239. https://doi.org/10.1016/j.rser.2015.10.156

Greening B, Azapagic A (2012) Domestic heat pumps : life cycle environmental impacts and potential implications for the UK. Energy 39(1):205–217. https://doi.org/10.1016/j.energy.2012.01.028

Guo H, Wang Y, Gao W, Li Z (2019) Performance evaluation of solar-air source heat pump hot water system in different climate zones. J Refrig 40:45–50. https://doi.org/10.3969/j.issn.0253-4339.2019.04.045

Hang Y, Du L, Qu M, Peeta S (2013) Multi-objective optimization of integrated solar absorption cooling and heating systems for medium-sized office buildings. Renew Energy 52:67–78. https://doi.org/10.1016/J.RENENE.2012.10.004

He G, Zheng Y, Wu Y, Cui Z, Qian K (2015) Promotion of building-integrated solar water heaters in urbanized areas in China: experience, potential, and recommendations. Renew Sustain Energy Rev 42:643–656. https://doi.org/10.1016/J.RSER.2014.10.044

Hong S, He G, Ge W, Wu Q, Lv D, Li Z (2019) Annual energy performance simulation of solar chimney in a cold winter and hot summer climate. Build Simul 12(5):847–856. https://doi.org/10.1007/s12273-019-0572-y

Hou Y, Yang B, Zhang S, Qi Y, Yu X (2022) 4E analysis of an integrated solar-biomass heating system: a case study in rural housing of Northern China. Sustain Energy Technol Assessments 53:102794. https://doi.org/10.1016/J.SETA.2022.102794

Huang Y, Cai M, Yan H (2014) The distributive character and compartment analysis of solar energy resources in Zhejiang Province Huang. Bull Sci Technol 30(5):78–85 (http://doi.org/10.13774/j.cnki.kjtb.2014.05.014)

Li D, Peng H, Qin X, Liang X, MA X, Huang Y. (2022) Research on Solar Energy Application Optimization Design of High-Density Urban Commercial Buildings in the Pearl River Delta Based on Carbon Audit. Build Energy Effic 50:80–87. https://doi.org/10.3969/j.issn.2096-9422.2022.11.014

IEA (2021) Achieving Net Zero Electricity Sectors in G7 Members. Retrieved https://www.iea.org/reports/achieving-net-zero-electricity-sectors-in-g7-members

IEA (2022a) Solar PV. IEA 1. Retrieved https://www.iea.org/reports/solar-pv

IEA (2022b) Solar Thermal Technologies Deployed in around 400 Million Dwellings by 2030. Retrieved https://www.iea.org/reports/solar-thermal-technologies-deployed-in-around-400-million-dwellings-by-2030

Joshi SS, Dhoble AS (2018) Photovoltaic -Thermal Systems (PVT): technology review and future trends. Renew Sustain Energy Rev 92:848–882

Kalogirou SA, Karellas S, Badescu V, Braimakis K (2016) Exergy analysis on solar thermal systems: a better understanding of their sustainability. Renew Energy 85:1328–1333. https://doi.org/10.1016/J.RENENE.2015.05.037

Kamel RS, Fung AS, Dash PRH (2015) Solar Systems and their integration with heat pumps: a review. Energy Build 87:395–412

Kant K, Pitchumani R (2022) Advances and opportunities in thermochemical heat storage systems for buildings applications. Appl Energy 321:119299. https://doi.org/10.1016/J.APENERGY.2022.119299

Kuhn TE, Erban C, Heinrich M, Eisenlohr J, Ensslen F, Neuhaus DH (2021) Review of technological design options for building integrated photovoltaics (BIPV). Energy Build 231:110381. https://doi.org/10.1016/J.ENBUILD.2020.110381

Liu *et al. City and Built Environment*   (2023) 1:16

Page 21 of 21

Klein SA (2016) TRNSYS 17: A Transient System Simulation Program. Univ Wisconsin-Madison. http://www.trnsys.com/

Leonforte F, Miglioli A, Del Pero C, Aste N, Cristiani N, Croci L, Besagni G (2022) Design and Performance Monitoring of a Novel Photovoltaic-Thermal Solar-Assisted Heat Pump System for Residential Applications. Appl Therm Eng 210(March). https://doi.org/10.1016/j.applthermaleng.2022.118304

Lerch W, Heinz A, Heimrath R (2015) Direct use of solar energy as heat source for a heat pump in comparison to a conventional parallel solar air heat pump system. Energy Build 100:34–42. https://doi.org/10.1016/J.ENBUILD.2015.03.006

Lu J, He G, Mao F (2020) Solar Seasonal Thermal Energy Storage for Space Heating in Residential Buildings: Optimization and Comparison with an Air-Source Heat Pump. Energy Sources, Part B Econ Plan Policy 279–96. https://doi.org/10.1080/15567249.2020.1786192

Lu J, Tang Y, Li Z, He G (2021) Solar Heat Pump Configurations for Water Heating System in China. Appl Therm Eng 187. https://doi.org/10.1016/j.applthermaleng.2021.116570

Ma Q, Chen X, Wang X, Gao W, Wei X, Fukuda H (2021) A Review of the Application of Sunspace in Buildings. Energy Sources Part A Recover Util Environ Eff. https://doi.org/10.1080/15567036.2021.1963884

Mahon D, Henshall P, Claudio G, Eames PC (2020) Feasibility Study of $MgSO_4$ + Zeolite Based Composite thermochemical energy stores charged by vacuum flat plate solar thermal collectors for seasonal thermal energy storage. Renew Energy 145:1799–1807. https://doi.org/10.1016/J.RENENE.2019.05.135

Martín-Chivelet N, Kapsis K, Wilson HR, Delisle V, Yang R, Olivieri L, Polo J et al (2022) Building-Integrated Photovoltaic (BIPV) Products and Systems: A Review of Energy-Related Behavior. Energy Build 262:111998. https://doi.org/10.1016/J.ENBUILD.2022.111998

MOHURD (2018) Technical Standard for Solar Water Heating System of Civil Buildings

MOHURD (2019) Standard for Design of Building Water Supply and Drainage

Pedraza J M. (2022) Solar Energy for Electricity Generation. In: Non-Conventional Energy in North America, p 137–74. https://doi.org/10.1016/B978-0-12-823440-2.00006-8

Qu M, Li T, Deng S, Fan Y, Li Z (2017) Improving defrosting performance of cascade air source heat pump using thermal energy storage based reverse cycle defrosting method. Appl Therm Eng 121:728–736. https://doi.org/10.1016/J.APPLTHERMALENG.2017.04.146

Sabiha MA, Saidur R, Mekhilef S, Mahian O (2015) Progress and latest developments of evacuated tube solar collectors. Renew Sustain Energy Rev 51:1038–1054. https://doi.org/10.1016/J.RSER.2015.07.016

Sadeghi H, Ijaz A, Singh RM (2022) Current Status of Heat Pumps in Norway and Analysis of Their Performance and Payback Time. Sustain Energy Technol Assessments 54(October):102829. https://doi.org/10.1016/j.seta.2022.102829

Shen W, He J, Yao S (2021) Green industrial policy in the post grid parity Era: governing integrated solar+ projects in China. Energy Policy 150:112129. https://doi.org/10.1016/J.ENPOL.2020.112129

Sifnaios I, Jensen AR, Dannemand M, Dragsted J (2021) Demonstration of a Domestic Photovoltaic-Thermal (PVT)-Heat Pump System, Performance Simulation, and Economic Analysis for Different Climates. Proc - ISES Sol World Congr 2021:588–99. https://doi.org/10.18086/swc.2021.26.03

Sovacool BK, Martiskainen M (2020) Hot transformations: governing rapid and deep household heating transitions in China, Denmark, Finland and the United Kingdom. Energy Policy 139(February):111330. https://doi.org/10.1016/j.enpol.2020.111330

Standardization administration (2015) Minimum Allowable Values of Energy Efficiency and Energy Efficiency Grades for Water Chillers

Sun Q, Wang Y, Cheng Z, Wang J, Zhao P, Dai Y (2020) Thermodynamic and economic optimization of a double-pressure organic rankine cycle driven by low-temperature heat source. Renew Energy 147:2822–2832. https://doi.org/10.1016/J.RENENE.2018.11.093

Ucar A, Inalli M (2008) Thermal and economic comparisons of solar heating systems with seasonal storage used in building heating. Renew Energy 33(12):2532–2539. https://doi.org/10.1016/J.RENENE.2008.02.019

Umair MM, Zhang Y, Iqbal K, Zhang S, Tang B (2019) Novel Strategies and Supporting Materials Applied to Shape-Stabilize Organic Phase Change Materials for Thermal Energy Storage–A Review. Appl Energy 235:846–873. https://doi.org/10.1016/J.APENERGY.2018.11.017

Vijay A, Hawkes A (2019) Demand side flexibility from residential heating to absorb surplus renewables in low carbon futures. Renew Energy 138:598–609. https://doi.org/10.1016/J.RENENE.2019.01.112

Yu L, Wu S, Jiang L, Ding B, Shi X (2022) Do More efficient buildings lead to lower household energy consumption for cooling? Evidence from Guangzhou. China Energy Policy 168:113119. https://doi.org/10.1016/J.ENPOL.2022.113119

Yang Y, Lu B, He T, Zhang X, Wang B. (2018) Investigation on Carbon Emission of Heating System in Beijing Rural Regions. Build Sci 34:87–91. https://doi.org/10.13614/j.cnki.11-1962/tu.2018.12.15

Zhang AH, Sirin SM, Fan C, Bu M (2022a) An analysis of the factors driving utility-scale solar PV Investments in China: How Effective Was the Feed-in Tariff Policy? Energy Policy 167:113044. https://doi.org/10.1016/J.ENPOL.2022.113044

Zhang Q, Zhang L, Nie J, Li Y (2017) Techno-economic analysis of air source heat pump applied for space heating in Northern China. Appl Energy 207:533–542. https://doi.org/10.1016/J.APENERGY.2017.06.083

Zhang S, He Y (2013) Analysis on the development and policy of solar PV Power in China. Renew Sustain Energy Rev 21:393–401. https://doi.org/10.1016/J.RSER.2013.01.002

Zhang T, Zhang S, Qu J (2022) The Impact of China's Carbon Neutrality Target on Its Energy Consumption Structure by 2050. Energy Sources, Part B Econ Planning, Policy 17(1). https://doi.org/10.1080/15567249.2022.2088896

Zheng C (2021) Observational multi-time scales temporal variations in water temperature of lake Taihu and its influencing factors. Sci Technol Eng 21:4793–4800

Publisher's Note